Journal of Hazardous Materials 491 (2025) 137992

Contents lists available at ScienceDirect

Journal of Hazardous Materials

journal homepage: www.elsevier.com/locate/jhazmat

Fission gas trapped in Chornobyl fuel microparticles reveals details of reactor operations

Laura Leifermann [a,*], Greg Balco [b], Autumn Roberts [b], Manuel Raiwa [b], Paul Hanemann [a], Tobias Weissenborn [a], David Ohm [a], Martina Klinkenberg [c], Michael Savina [b], Darcy van Eerten [a], Felix Brandt [c], Brett H. Isselhardt [b], Clemens Walther [a]

[a] Institute of Radioecology and Radiation Protection, Herrenhäuserstr. 2, Hannover 30419, Germany
[b] Lawrence Livermore National Laboratory, Nuclear and Chemical Sciences Division, 7000 East Ave, Livermore, CA 94551, USA
[c] IFN-2: Nuclear Waste Management, Forschungszentrum Jülich, Wilhelm-Johnen-Str., Jülich 52428, Germany

HIGHLIGHTS

- FIB-cut weathered micron sized nuclear fuel particles show a closed pore structure.
- Gas measurements on hot particles that are over 30 years old with low burnup show gas inclusions of fissiogenic Xe and Kr.
- The age of these particles could be dated to a few years before the Chernobyl accident.
- Using RIMS measurements of Zr, particles within a pellet could be assigned to a possible origin.

GRAPHICAL ABSTRACT

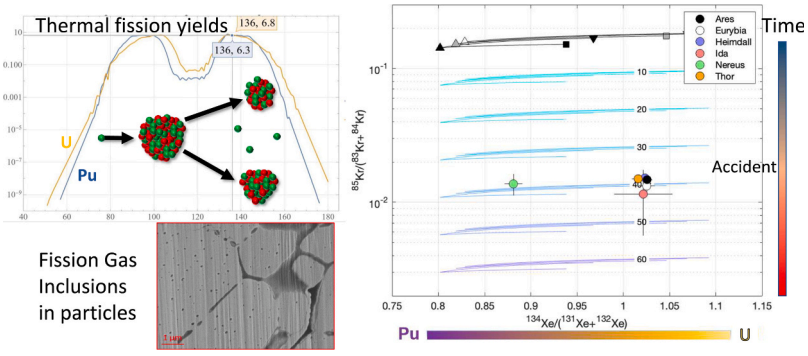

ARTICLE INFO

Keywords:
Single hot particle analysis
Noble gas spectroscopy
Chornobyl
RIMS
RBMK
FIB

ABSTRACT

The isotopic ratios of fission gas would provide important source information of a nuclear fuel sample found in the environment. However, it is believed that during a reactor accident like Chornobyl all fission gas is lost and that the radioactive particles found in the Chornobyl Exclusion Zone today are depleted in gases by the initial explosion and subsequent fire. We disprove this hypothesis by detection and analysis of trapped krypton and xenon in these particles. Our analysis of krypton and xenon isotopes by noble gas mass spectroscopy in combination with resonance ionization mass spectrometry establishes that important information about reactor operations like age, neutron flux and plutonium fission fraction can still be reconstructed from individual micrometer-sized particles even after decades of weathering in the environment.

Abbreviations: EDS, Energy Dispersive Spectroscopy; FIB, Focused ion beam; IAEA, International Atomic Energy Agency; RIMS, Resonant Ion Mass Spectrometry; SEM, Scanning Electron Microscopy; SIMS, Secondary Ion Mass Spectrometry; SNMS, Secondary Neutrals Mass Spectrometry; UN, United nations.

* Correspondence to: Leibniz University Hannover Institute of Radioecology and Radiation Protection, Herrenhaeuserstr. 2, Hannover 30419, Germany.
E-mail address: leifermann@irs.uni-hannover.de (L. Leifermann).

https://doi.org/10.1016/j.jhazmat.2025.137992
Received 19 December 2024; Received in revised form 24 February 2025; Accepted 16 March 2025
Available online 21 March 2025

1. Introduction

Various radioactive isotopes are released during the explosion and graphite fire at the Chornobyl reactor accident in 1986. Both the United nations (UN) and the International Atomic Energy Agency (IAEA) state, that this event resulted in the complete release of Krypton, (e. g. 33 PBq ^{85}Kr) and Xenon (e.g. 6500 PBq ^{133}Xe) inventory of the reactor [12,30]. Additionally, fragments of the nuclear fuel itself were dispersed into the environment, predominantly within the confines of the Chornobyl Exclusion Zone, although the finest particles were dispersed across Europe [13]. These fuel remnants, often referred to as hot particles, predominantly comprise uranium along with fission and breeding products, exhibiting diverse morphologies and resilience to environmental conditions [18]. Most identified hot particles fall within the micrometer range [4,14,16,17,27,28].

Non-destructive analytical techniques such as Scanning Electron Microscopy (SEM), Energy Dispersive Spectroscopy (EDS), and quasi-non-destructive static Secondary Ion Mass Spectrometry (SIMS), Secondary Neutrals Mass Spectrometry (SNMS) and Resonant Ion Mass Spectrometry (RIMS) have been essential in surface-level characterization of these particles [3,23]. Furthermore, gamma measurements can be used to quantify the activity of some isotopes within the particles [18]. In this work, we improve upon existing characterization of particle surfaces by (i) dissecting particles to reveal their unweathered internal cores, and (ii) extracting fission-produced noble gases from particles as a means of diagnosing reactor operations from fission products. The use of a focused ion beam (FIB) enables the examination of the unweathered internal material. Approximately 15 % of all fission products generated during reactor operation manifest as gaseous elements [5]. Notably, gases like krypton and xenon exhibit minimal solubility in uranium dioxide, leading to their aggregation into bubble formations that coalesce into tunnel networks within the fuel [26]. Thus, fission gases are present both dissolved in oxide fuel at the site of production and in minuscule, nanometer- to micrometer-scale bubble inclusions [25,26].

However, investigations into fission gas content of microparticles have so far been limited to spent nuclear fuel particles prepared directly from research fuel samples [5]. The above measurements have yet to be tested on environmental samples or, specifically, on hot particles from Chornobyl. Important nuclear forensic information can be reconstructed by isotopic ratios from the fission gases krypton and xenon. This includes information about the fuel composition and burnup, neutron flux and spectrum, and the age of the sample via decay of ^{85}Kr [1].

2. Material and methods

2.1. Particle separation

The particles described in this study were extracted from soil and sediment samples collected in the Chornobyl exclusion zone in 2014 and 2017. For the analysis of particles without interfering background, they must be localized in soil samples and extracted on needles. For a detailed description of how this is done, refer to Leifermann et al. [18]. Five particles are prepared for cutting using FIB and six particles are prepared for the gas measurements.

2.2. Cutting particles using focused ion beam

The particle is prepared as described in Leifermann et al. so that it sticks firmly to the tip of a needle. A fresh needle is mounted onto a micromanipulator (KLEINDIEK NANOTECHNIK) in a focused ion beam (FIB) system (NVISION 40, ZEISS) at the Research center Jülich. The particle is positioned on a sample holder located on the sample plate, which allowed tilting of the sample. SEMGLUE is used to attach the second needle to the particle. Since this procedure has not previously been performed on particles, various currents are tested and adjusted to effectively cut through the particle. Once the particle is completely severed, the second needle is disengaged from the particle. Subsequently, one half of the particle is retained on each needle, facilitating examination of the particle's cross-section, while the other half remained available for additional measurements and analyses (fig. 1).

2.3. Sample preparation for noble gas measurements

For noble gas mass spectrometry measurements, the particles are removed from the needle tip and encapsulated within a tantalum foil, which is subsequently housed within a larger tantalum enclosure made by crimping a small segment of tubing (Fig. S1). This packaging is not gas-tight so that extracted noble gases are released for analysis. The enclosure is then placed under vacuum and heated with a 140 W, 970 nm diode laser that is coupled to an optical pyrometer in a control loop that adjusts laser power to achieve a specified temperature of the outer package. To prevent introduction of potential hydrocarbon interferences into the mass spectrometer, each particle was initially preheated to 800° C to combust the hydrocarbon glue used for particle handling, and evolved gas was pumped away without analysis. Samples were subsequently heated in a series of heating steps starting at 1000° C. After each heating step, evolved noble gases were purified by reaction with hot and cold getters and then introduced into a Nu Instruments 'Noblesse' mass spectrometer equipped with five Faraday cup detectors and five ion-counting discrete dynode multipliers. All stable xenon and krypton isotopes, plus ^{85}Kr, were measured on ion multipliers. The temperature of heating steps was subsequently increased in 50–100° C increments until sufficient xenon and krypton had been extracted for precise isotope ratio analysis. At this point heating was halted to minimize possible damage to particles and preserve them for additional analyses, so no attempt was made to quantitively extract all fission gas present. Observed Xe and Kr signals were then corrected for any atmospheric contribution by assuming that all ^{80}Kr and ^{129}Xe observed are atmospheric, and correcting other isotope signals according to their atmospheric ratios. In most cases atmospheric corrections were less than 5 % for major isotopes. Finally, amounts of Xe and Kr isotopes released in all heating steps for each sample were summed to calculate mean isotope ratios for all fission gas released from that sample. The complete step-degassing data are reported in table S5 in the supplementary material.

2.4. RIMS measurements after noble gas measurements

Following the measurements, the particle must be localized again. This is achieved by carefully unfolding the foil and applying a very dilute sugar solution onto it. The approximate position of the particle is continuously monitored using a Geiger Müller Counter (GMC). Subsequently, the foil is inserted into a SEM to precisely locate the particles on the surface. The particle can then be further analyzed using RIMS at Lawrence Livermore National Laboratory (LLNL). For the analysis of zirconium as well as uranium and plutonium, the methodologies are described by [24,32].

3. Results

In this work, five particles are successfully cut using FIB and six particles are analyzed using noble gas mass spectrometry. The particles are labeled with names. An overview of the gamma activities of the with noble gas mass spectrometry analyzed particles can be found in Table 1.

While EDS measurements of particles' surfaces reveal features like molten zirconium from the fuels cladding, no such inhomogeneous features on the micrometer size were observed within the particles (Fig. S2 Supplement). The important feature shown in the SEM images in Fig. 2 is the intact pore structure that permeates the entire particle regardless of the apparent surface structure. The pores and grain boundaries are both sealed and isolated from one another, preventing the escape of any gas. Due to the small size of these gas bubbles, they are

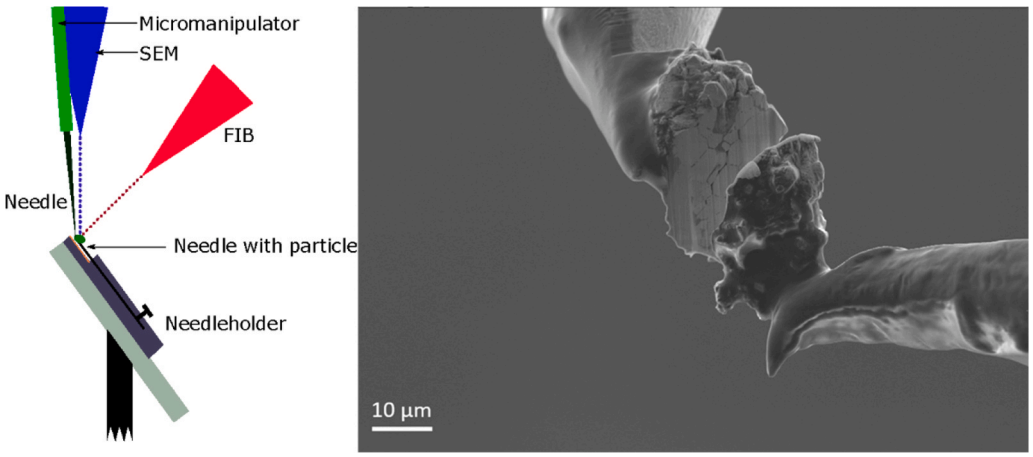

Fig. 1. Cutting process with two needles at one particle. Left: schematic diagram of the cutting process. Right: Cut particle with one half of the particle on one needle.

Table 1
The table shows the particles measured using noble gas mass spectrometry. The activity is given in Bq at the time of measurement. The morphology estimated from the structure in the SEM image and the main elements measured in the EDS are also shown. It is evident that the particles exhibit adhesions of various elements on their surface, including Fe and S. The nomenclature of the particles is employed for the purpose of identification.

Particle	Date of Measurement	^{137}Cs [Bq]	^{241}Am [Bq]	Main elements	Morphology
Ares	18th March 2019	150(1)	7.6(1)	U, Zr, Fe	$U_XZr_YO_Z$
Eurybia	20th January 2023	19.2(1)	0.82(1)	U	UO_2
Heimdall	03th August 2021	10.1(1)	0.51(1)	U	-
Ida	04th August 2021	0.09(1)	1.0(2)	U, Fe, S	UO_2
Nereus	12th August 2022	28.8(1)	1.68(2)	U	UO_{2+X}
Thor	17th August 2022	19.3(1)	1.36(2)	U	UO_2

only evident on smooth surfaces which necessitates the FIB cut. This pore structure spanning from a few micrometers down to the nanometer scale is the result of the produced fission gases during reactor operation. Such voids are commonly encountered in spent nuclear fuel and grow with higher burnup [26].

3.1. Noble gas measurements

As the temperature in the reactor core at meltdown is estimated at 2500 °C, the presence of fission gas released by heating to the 1000° - 1200 °C range indicates that the analyzed particles must have been ejected from the reactor well before peak core temperatures were reached. However, the presence of zirconium coatings on some particles that contain noble gases indicates at least brief exposure to temperatures at or above the melting point of Zr (1800 °C) [8,17]. The presence of noble gases in these particles indicates that they are not readily released from oxide fuels, even in extreme conditions of fire, explosion, and exposure to environmental weathering over long periods of time.

Particles without a Zr-cladding are also released. The Zr-cladding of the Ares particle, for example, may be interpreted as part of the molten cladding material, consisting of a zirconium alloy, and thus of natural isotope ratios. It cannot be ruled out that the uranium itself was not exposed to such high temperatures and that the Zr only melted on top of it. The measured particles were probably not exposed to the high temperatures in the reactor, as it would not have been possible to measure krypton, xenon and cesium under such conditions. The presence of burnup dependent fissiogenic Zr can be discerned in all particles, wherein this element is integrated into the particle's structural composition. Nevertheless, the surface of the particle may also exhibit Zr originating from the Zr utilized in the cladding. Substantial quantities of gas are detected even within particles lacking visible surface pores. This finding validates statements made by Rest et al. [26] regarding the nanometer-scale size of these pores, which may be less discernible on rough surfaces. Consequently, these measurements confirm that the bubbles observed in the cutted particles contain fission gas. However, it has no environmental consequences because, firstly, the gas is safely trapped in the fuel, secondly, large parts of it have already decayed in the fuel itself. Thirdly, even if it were released, the high radioactivity is in the xenon radioisotopes, which decayed a long time ago due to its short half-life and the remaining noble gases are inert and have only little effect on human body.

3.1.1. Source

Analysis of the isotope ratios of xenon and krypton can clarify the specific parent isotopes that underwent nuclear fission due to the different thermal fission yields for ^{235}U and ^{239}Pu. The ratio ^{86}Kr/(^{83}Kr+^{84}Kr) is used because ^{83}Kr+^{84}Kr is insensitive to neutron capture after production and thus reflects the fission yield ratio rather than the neutron flux [1]. The ratio ^{134}Xe/(^{131}Xe+^{132}Xe) adheres to analogous principles. Notably, these fission yield ratios exhibit significant divergence between uranium and plutonium fission, this makes them valuable for isotopic characterization [1,5]. The different fission yields for Pu-fission of ^{86}Kr (0.761) and ^{83}Kr+^{84}Kr (0.484 +0.294) result in a ratio of one for pure Pu fission. If there is more U fission, the fission yield for ^{86}Kr (1.96) increases much more than for ^{83}Kr+^{84}Kr (0.996 +0.552) and the ratio shifts to 1.3 (Magill, 2018) (Magill, 2018). The same assumptions and justifications of ^{86}Kr/(^{83}Kr+^{84}Kr) also apply to ^{134}Xe/(^{131}Xe+^{132}Xe). With the fission yields for ^{235}U, the ratio of ^{134}Xe/(^{131}Xe+^{132}Xe) for pure uranium fission is 1.07 and for ^{239}Pu with a pure plutonium fission is the ratio 0.75 (Fig. 3).

In four of the measured particles (Ares, Eurybia, Heimdall, Thor) in Fig. 4 the resulting fission gases are mainly caused by uranium fission. This also fits very well with the fuel used in the reactor, which has an enrichment level of approximately 2 % ^{235}U and a low burnup of around 11 GWd/tU [9,15,31,33]. The substantial error bars observed for Ida stem from the limited gas release during these measurements which is consistent with its small size, low ^{137}Cs concentration, and the likelihood of variable loss of included fission gas during ejection in the explosion. Consequently, it is unsurprising that the recorded gas quantities are modest, resulting in high uncertainties.

The isotopic composition of the Nereus particle deviates significantly from that of the other microparticles. This is far outside the expected range and indicates significantly more ^{239}Pu fission in the production of

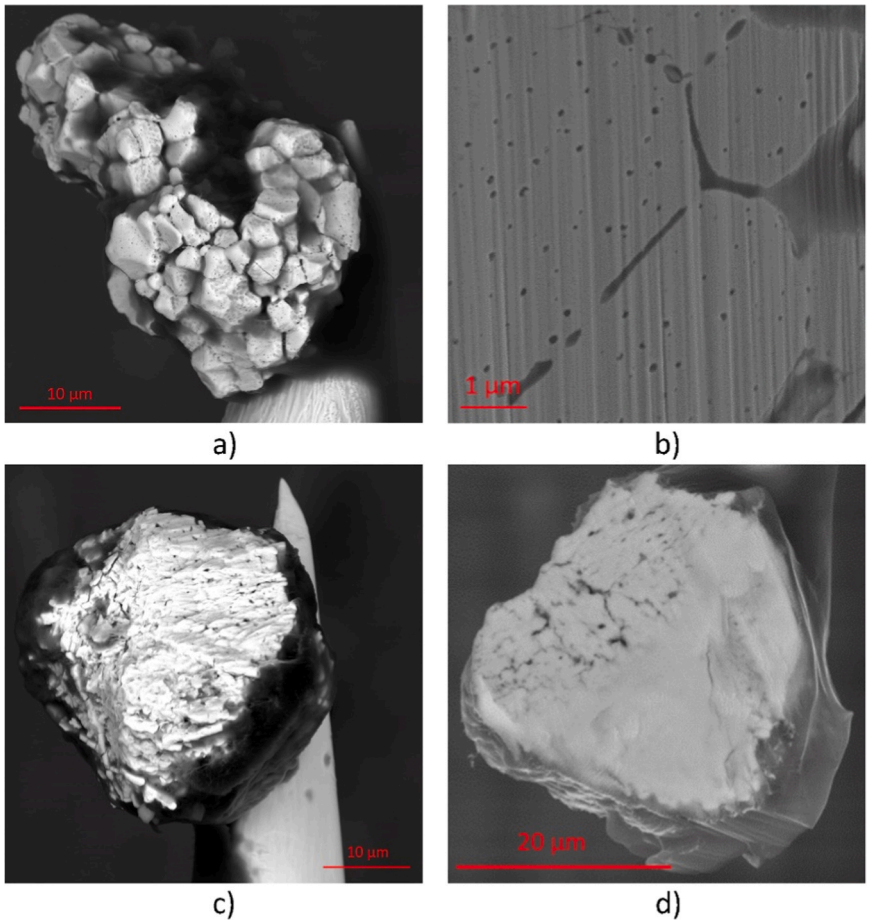

Fig. 2. a) Particle structure of Momos before cutting. b) Pore structure of Momos after cutting with FIB c) Particle Mjöllnir with weathering before cutting, d) Pore structure of weathered particle Mjöllnir.

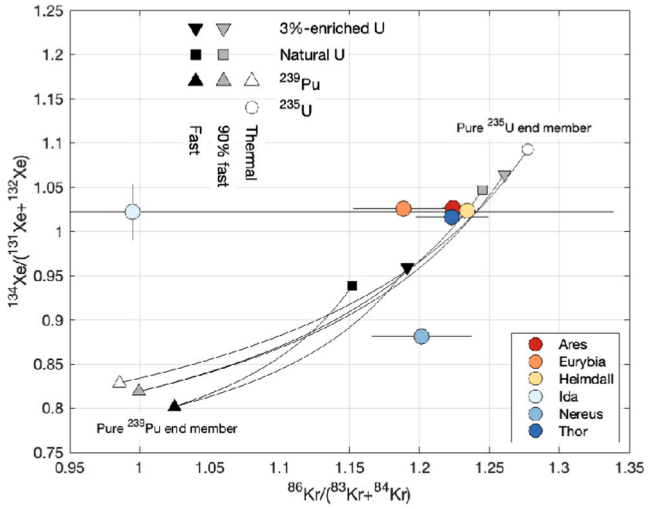

Fig. 3. The plotted $^{86}Kr/(^{83}Kr+^{84}Kr)$ to $^{134}Xe/(^{131}Xe+^{132}Xe)$ ratios serve as indicators of the likely sources of these isotopes from nuclear fission processes. Reference lines corresponding to the variation of the initial ratios during production in a range of fission sources on the figure for comparison [1]. The extremities of calculated values are highlighted using gray and black triangles and boxes, delineating the range of possible ratios. Each colored dot on the plot represents a measured ratio of $^{86}Kr/(^{83}Kr+^{84}Kr)$ to $^{134}Xe/(^{131}Xe+^{132}Xe)$, providing empirical data points within the context of the plotted theoretical calculations.

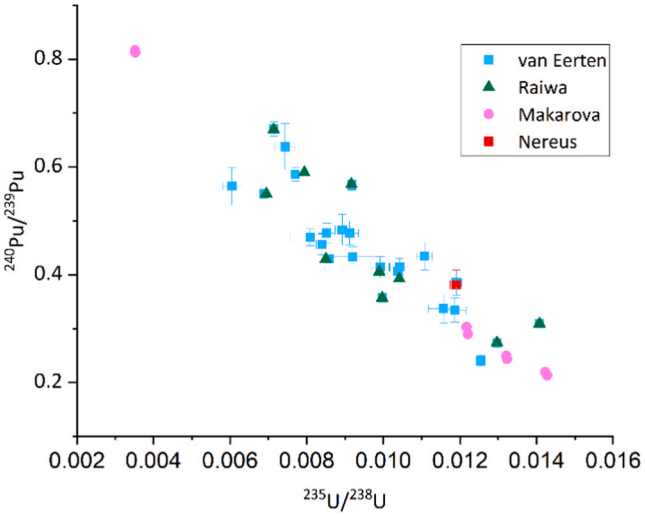

Fig. 4. The isotope ratios of $^{235}U/^{238}U$ and $^{240}Pu/^{239}Pu$ were measured with RIMS and SNMS. The data from van Eerten et al. [32], Raiwa [22] and Makarova et al. [20] were used. Nereus lies exactly in the trend of the particles and is not an outlier. The particle has an average burn-up and the U and Pu values provide no indication of a particle that was formed from other fuels.

the fission gases. Both, the krypton and the xenon ratios are in the range of more plutonium fission, although the xenon values differ more.

The SIMS and SNMS results suggest that the isotope ratios U and Pu

of Nereus are not unusual. They are exactly in line with the trend of the particles measured in various previous studies by van Eerten [32] and Raiwa [22] and the data published by Makarova et al. [20]. The particle is in the medium burnup range.

3.1.2. Age dating

Fig. 5 indicates how the date when the particles were irradiated can be inferred from the Kr and Xe isotope composition. The initial $^{85}Kr/(^{83}Kr+^{84}Kr)$ ratio varies somewhat with the fissioning material, but can be estimated by its correlation with the stable isotope ratios $^{134}Xe/(^{131}Xe+^{132}Xe)$ or $^{86}Kr/(^{83}Kr+^{84}Kr)$, which are also diagnostic of the fission source. Measured $^{85}Kr/(^{83}Kr+^{84}Kr)$ ratios are much less than estimated initial ratios due to radioactive decay, which allows an estimate of the date of irradiation. All particles have indistinguishable ^{85}Kr dates ranging from October, 1981 + /- 8 years to November, 1985 + /- 1 year, with a median age of July, 1985. This is consistent with the typical residence time of Chornobyl fuel rods in the reactor was 1100–1200 days [2].

3.1.3. Thermal neutron flux densities

Isotope ratios involving ^{136}Xe can be used to estimate thermal neutron flux densities in the reactor. ^{136}Xe is produced through neutron capture by ^{135}Xe, which boasts a notably high thermal neutron capture cross-section of 2.65 * 10^6 b. The conversion of ^{135}Xe to ^{136}Xe scales with the thermal neutron flux density. This relationship underscores the utility of ^{136}Xe as a sensitive indicator of neutron activity under varying operational conditions. The values for all particles except Nereus are usual for the RBMK reactor and correspond to the expected values [11, 21]. Noticeable different is the Nereus particle with significantly lower values for the thermal neutron flux densities (Fig. 6).

3.2. Comparison with RIMS measurements

The isotopic ratios of zirconium were also measured by resonance ionization mass spectrometry (RIMS). The Zr originates from two different sources: Zirconium produced by fisson (fissiogenic) is

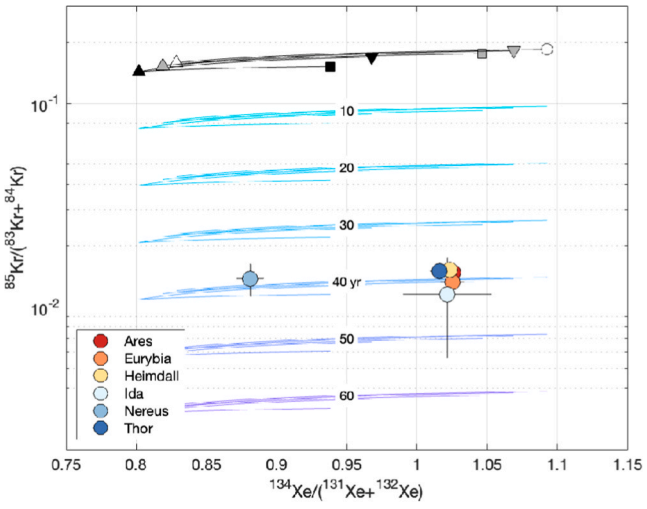

Fig. 5. The age of the particles is shown in the figure. The source of the fission is again indicated on the X-axis. The ratio of the radioactive ^{85}Kr ($T_{1/2}$=10,74 years) to the stable $^{83}Kr+^{84}Kr$ is given on the Y-axis. From this, the age of the particles can be easily calculated using the decay law. The black lines give the fission yields, which is the initial isotope ratio at formation, for various fission sources, with the same color-coding as in Fig. 4. The colored dots are the measured particles. The horizontal lines indicate the different decades to which the isotope ratios can be calculated back. All particles are calculated to have a similar age of approximately 40 years. The position of Nereus shows again that it must come from a different source of fission than the other particles.

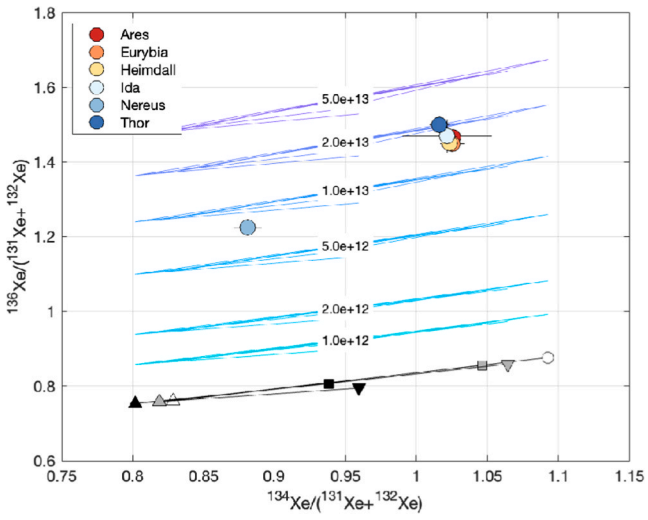

Fig. 6. The Xe isotope ratios are plotted on the X-axis, as in Fig. 4, which indicate the source of the fission gases. The Y-axis shows the ^{136}Xe isotope ratios, which are normalized to the same isotopes as for ^{134}Xe. The ^{136}Xe is an indicator of the thermal neutron flux densities in the reactor. The black lines give the fission yields, which is the initial isotope ratio at formation, for various fission sources, with the same color-coding as in Fig. 4. while horizontal lines represent various calculated thermal neutron flux densities, compare to Fig. 4. The majority of data points cluster around the 2 * $10^{13}cm^{-2}s^{-1}$ range, which is relatively low but characteristic of RBMK reactors. Nereus exhibits a distinct deviation from other particles, indicating significantly lower thermal neutron flux exposure compared to the rest of the dataset.

incorporated into the U matrix and distributed homogeneously over the particles' entire UO_2 matrix. Natural Zr is used for the fuel cladding. Hence, Zr at the surface of the particles has natural isotope ratios and little or no fissiogenic zirconium isotopes. Analogous to the noble gas measurements the different fission yields are used to estimate the fraction of ^{239}Pu fissions. The method is described in detail by [24]. In brief, the $^{93}Zr/^{91}Zr$ and $^{94}Zr/^{91}Zr$ ratios shift from 1.10 and 1.09 for 100 % ^{235}U fission towards 1.6 and 1.77 with increasing ^{239}Pu fissions respectivly. Interference from non-fissiongenic zirconium is ruled out by comparing the results of both isotope pairs. In this case the $^{93}Zr/^{91}Zr$ would drop as ^{93}Zr is pure anthropogenic and not found in natural zirconium while the ratio of $^{94}Zr/^{91}Zr$ shifts towards its natural abundance ratio of 1.55. These shifts lead to a discrepancy in the calculated ^{239}Pu fission fraction which indicate contamination with natural zirconium. In this study this was the case for the particle Ares which clearly shows cladding fused to its surface (Fig S3.).

The results for the remaining five particles are given in Fig. 7. All particles show about 10 % fission fraction from ^{239}Pu which is comparable to the calculated value by the noble gas measurements (For $^{134}Xe/(^{131}Xe+^{132}Xe)$ all particles around 20 %, but Nereus 63 %, $^{86}Kr/(^{83}Kr+^{84}Kr)$ more differences between the particles from 11 % to 31 % and Ida, which is not evaluable with the large uncertainties). One particle (Ida) shows a lower fission fraction consistent with 0 for the ^{93}Zr based value. As the value is outside the 1-sigma uncertainty of the ^{94}Zr value this is most likely a result of a minor natural zirconium interference. Nereus shows smaller spots of zirconium, which could be cladding material with neutral zirconium isotopic ratios in the element mapping, which can also reduce the apparent $^{93}Zr/^{91}Zr$ ratio.

4. Discussion

Analysis of the cut edges has provided deeper insights into the nature of fuel fragments from Chornobyl, particularly highlighting the presence of gas inclusions within the particles regardless of surface structure and environmental weathering. The predominant closed porosity of the

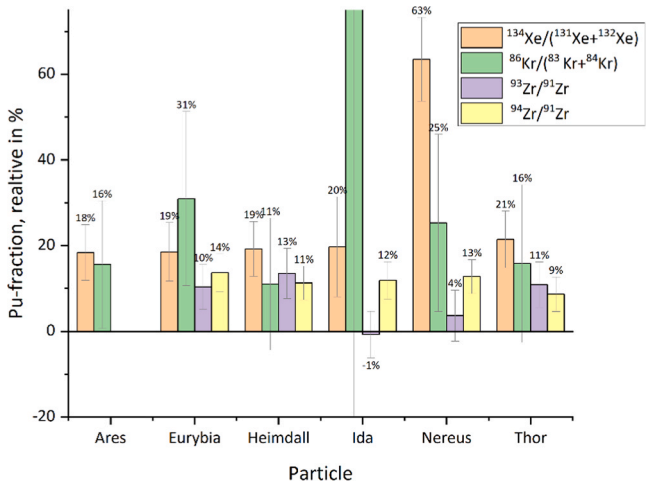

Fig. 7. The isotope ratios of $^{86}Kr/(^{83}Kr+^{84}Kr)$ and $^{134}Xe/(^{131}Xe+^{132}Xe)$ as well as of fissiogenic $^{93}Zr/^{91}Zr$ and $^{94}Zr/^{91}Zr$ are shown. The fissiogenic Zr is built into the UO_2 matrix of the particles in contrast to the Zr cladding from the fuel rods. The proportion of ^{239}Pu fission is calculated from these ratios and plotted on the y-axis for the respective isotope ratios and particles. No Zr ratios could be measured for Ares, as it has a Zr cladding with natural Zr isotope ratios. The fissiogenic Zr was measured for the other 5 particles. The error bars for Ida are particularly large, as hardly any gas could be measured here.

particles results in the retention of the gas. The gas inclusions in the particles can originate from the detected pores or be incorporated into the UO_2 matrix. These particles contain significant amounts of noble gases that persist decades after the Chornobyl accident which is in direct disagreement with previous reports where it was stated that all fission gas was lost from the core [30].

Plutonium is generated over time within a reactor through neutron capture by uranium and subsequent decay processes. This transformation results in the formation of plutonium with typically small quantities within the reactor. A review of the data from the noble gas measurements reveals that, with one exception, the data agree on their assessment of the fuel burnup, origin, thermal neutron flux, etc. The sole particle that fails to meet expectations is Nereus. There is no evidence that plutonium was contained as a raw material in the Chornobyl reactor [9,10,31]. It can be definitively stated that mixed oxide fuel (MOX) was not used in the Chornobyl incident, as the U and Pu isotope ratios of Nereus are clearly consistent with those observed in Chornobyl and the other measured particles [6]. At the top and bottom ends of the fuel rod, the neutron fluxes are significantly lower than in the middle of the fuel rod. In addition, the neutron flux densities decrease from the outside to the inside of the reactor, so an additional factor here could be not only the upper edge of the fuel rod, but also the radial center of the reactor. The higher $^{132}Xe/^{131}Xe$ ratio of Nereus indicates a that the particle experienced more fluence and thus a longer time in the reactor. So, on the one hand we have the values of ^{134}Xe, which indicate a high burnup, and on the other hand the ratio of $^{136}Xe/(^{131}Xe+^{132}Xe)$, which indicates a low neutron flux, thus low burnup and a longer time in the reactor. Also, the $^{235}U/^{238}U$ ratios of 1.22 % indicate, that this particle has a very low neutron flux. A prolonged residence time and/or an edge position in a relatively low neutron flux region of the reactor can account for the majority of the observations.

The possibility of an adherent contamination of Xe can be excluded, because negligible ^{129}Xe was observed. The ^{129}Xe is the indicator for contamination with atmospheric xenon, since this is not formed in the reactor due to the long half-life of the parent nuclide ^{129}I ($T_{1/2}$=1.57 *10^7 years) [19]. The origin of the Xe isotope ratios is evident for all particles, with the exception of Nereus, for which a definitive explanation remains elusive.

The measured isotope ratios and the calculated age of the particles are consistent with the literature on the Chornobyl reactor accident [20,30]. There is no radiological hazard from the noble gases that have not yet been released or are being released slowly. The calculated age of the particles clearly dates them into the irradiation period before the accident. It is unnecessary to determine the age of the particles from Chornobyl, as the release period is known. However, determining the age of other radioactive particles of unknown origin or from several sources is beneficial for further research. While such a radiochronology analyses is also possible by the isotopic pair $^{90}Sr/^{88}Sr$ [29,32] this gives an important second measurement, which were done for Ares and Heimdall by van Eerten et al. [32] and calculates to be 1985 ± 1, therefore the same age as the ^{85}Kr measurements for these two particles. Here the produced fission gas is partially lost during the irradiation period while the strontium does not suffer from this effect [1]. There is no radiological hazard from the up to 1.5 % of noble gases in particles in the environment that have not yet been released or are being released slowly. 98,5 % of the original inventory in Chornobyl remained in the shelter. The correct identification of a sample from the edge of a pellet is of paramount importance in nuclear forensics as its elemental and isotopic ratios differ dramatically from the average fuel pellet and thus would lead to wrong conclusions about the source of the sample [7,34]. The results after heating the particles give the same results and were thus confirmed by two different measuring devices RIMS and SNMS before and after heating. This validation underscores the reliability and robustness of the analytical approach employed in this study.

5. Conclusion

In summary, the measurements conducted have yielded significant success. Two novel methods for analyzing particles originating from Chornobyl have been established and will be utilized in future studies. The process of cutting the particles has been proven effective, enabling one half of them to serve as reference materials for future measurements. Analysis of the cut edges has provided deeper insights into the nature of fuel fragments from Chornobyl, particularly highlighting the presence of gas inclusions within the particles. Noble gas measurements carried out at LLNL have opened up new possibilities for studying µm-sized particles. These particles contain significant amounts of noble gases that persist decades after the Chornobyl accident. These measurements made it possible to identify whether the particles came from fission processes of uranium or plutonium. What is impressive is that the age of the particles could be determined to a specific time window before the accident happened, despite the small amounts of gas measured. Furthermore, reconstruction of thermal neutron flux densities within the reactor during operation is achieved based on these measurements. They are aligning well with calculated models. Additionally, RIMS measurements conducted post-heating of the particles to high temperatures have consistently provided results corroborated by two separate measurement devices. This validation underscores the reliability and robustness of the analytical approach employed in this study.

Outlook

Further studies on more particles from Chornobyl and on Nereus would help to unravel the puzzle of the unusual Xenon isotope ratios. It would also be interesting to investigate other particles with unusual isotope ratios to see if there could be more samples with possibly more Pu fission.

The noble gas measurements can also be carried out in the future on other sources. These measurements could explain the origin and history of unknown fuel samples. Other types of reactors should have different characteristic gas releases and should also be distinguishable from detonated nuclear weapons. Furthermore, more particles from Chornobyl should be examined in order to be able to better explain particles like Nereus and to increase the statistics.

Environmental implication

The detection of trapped fission gases like krypton and xenon, volatile fission products, in Chornobyl microparticles challenges previous assumptions that such gases were fully released at the high temperatures of the accident. This new process understanding suggests that long term environmental contamination by hot particles is more complex than initially thought. Understanding fission product entrapment and retention in these particles - and release even after decades- highlights potential long-term environmental impacts and the need for ongoing monitoring and analysis to assess ecological consequences accurately of long-lived radioactive pollutants in the ecosystem.

CRediT authorship contribution statement

van Eerten Darcy: Investigation. **Brandt Felix:** Writing – review & editing, Conceptualization. **Isselhardt Brett H.:** Supervision, Project administration. **Leifermann Laura:** Writing – original draft, Investigation, Conceptualization. **Walther Clemens:** Writing – review & editing, Supervision, Resources, Project administration. **Balco Greg:** Writing – review & editing, Visualization, Formal analysis, Data curation. **Roberts Autumn:** Methodology. **Raiwa Manuel:** Writing – review & editing, Investigation. **Hanemann Paul:** Investigation. **Weissenborn Tobias:** Investigation. **Ohm David:** Investigation. **Klinkenberg Martina:** Writing – review & editing, Investigation, Conceptualization. **Savina Michael:** Supervision, Project administration.

Declaration of Competing Interest

The authors declare that they have no known competing financial interests or personal relationships that could have appeared to influence the work reported in this paper.

Acknowledgements

Many thanks to Murat Güngor for his lab work at FIB at Research center Jülich. Part of this work was performed under the auspices of the U.S. Department of Energy by Lawrence Livermore National Laboratory under Contract DE-AC52–07NA27344. This is LLNL-JRNL-871676. Many thanks for the financial support from the Siebold-Sasse-Foundation, the SOLARIS project BMBF 2020 + 02NUK075A and the LISA project.

Appendix A. Supporting information

Supplementary data associated with this article can be found in the online version at doi:10.1016/j.jhazmat.2025.137992.

Data availability

Data will be made available on request.

References

[1] Balco, G., Conant, A.J., Reilly, D.D., Barton, D., Willett, C.D., and Isselhardt, B.H. Krypton-85 chronometry of spent nuclear fuel. Geochronology Discuss. 2024. https://doi.org/10.5194/gchron-6-571-2024.
[2] Bibilashvili, Yu.K., F.G. Reshetnikov, A.G. Ioltukhovsky. 1998. Status and development of RBMK fuel rods and reactor materials. 1998.
[3] Bosco, H., Hamann, L., Kneip, N., Raiwa, M., Weiss, M., Wendt, K., Walther, C., 2021. New horizons in microparticle forensics: actinide imaging and detection of 238Pu and 242mAm in hot particles. Sci Adv 7 (44), eabj1175, 2021.
[4] Bulgakov, A., Konoplev, A., Smith, J., Laptev, G., Voitsekhovich, O., 2009. Fuel particles in the Chernobyl cooling pond: current state and prediction for remediation options. J Environ Radioact 100 (4), 329–332, 2009.
[5] Cassata, W.S., Isselhardt, B.H., Conant, A.J., Charboneau, J., Carney, K.P., 2023. Noble gas constraints on spent fuel irradiation histories. J Radioanal Nucl Chem 332 (8), 3151–3159, 2023.
[6] Dawahrah, S. 1991. Increasing Plutionium Dispsition Rate in the Thermal Reactors (VVER AND RBMK). Vienna: IAEA, 1991. p. 552. 0074-1884.
[7] Desgranges, L., Pasquet, B., Valot, Ch, Roure, I., 2009. SIMS characterisation of actinide isotopes in irradiated nuclear fuel. J Nucl Mater 385 (1), 99–102, 2009.
[8] Devell, L., Tovedal, H., Bergström, U., Appelgreen, A., Chyssler, J., Andersson, L., 1986. Initial observations of fallout from the reactor accident at Chernobyl. Letters to nature, 321, 192–193, 1986.
[9] Gesellschaft für Reaktorsicherheit (GRS) mbH. Neue Erkenntnisse zum Unfall im Kernkraftwerk Tschernobyl. 1987. GRS-S-40.
[10] Gesellschaft für Reaktorsicherheit (GRS) mbH. Tschernobyl-Zehn Jahre danach. 1996. GRS - 121 Köln: s.n. p. 186.
[11] Gulshani, P., Dastur, A.R., Chexal, B., 1987. Stability analysis of spatial power distribution of the RBMK-100 reactor. Trans Am Nucl Soc 1987, 383–386.
[12] IAEA, 2006. Environmental consequences of the Chernobyl accident and their remediation: twenty years of experience. STI PUB 1239.
[13] IAEA-Report. 2011. Radioactive Particles in the Environment: Sources, Particle Characterization and Analytical Techniques. Vienna: s.n., 2011. 978-92-0-119010-9.
[14] Kashparov, V.A., Ahamdach, N., Zvarich, S.I., Yoschenko, V.I., Maloshtan, I.M., Dewiere, L., 2004. Kinetics of dissolution of Chernobyl fuel particles in soil in natural conditions. J Environ Radioact 72 (3), 335–353, 2004.
[15] Kashparov, V., Levchuk, S., Zhurba, M., Protsak, V., Khomutinin, Y., et al., 2018. Spatial datasets of radionuclide contamination in the Ukrainian Chernobyl exclusion zone. Earth Syst Sci Data 10, 339–353, 2018.
[16] Kashparov, V., Salbu, B., Levchuk, S., Protsak, V., Maloshtan, I., Simonucci, C., Courbet, C., Nguyen, H., Sanzharova, N., Zabrotsky, V., 2019. Environmental behaviour of radioactive particles from Chernobyl. J Environ Radioact . 208-209, 106025, 2019.
[17] Kashparov, V., Yoschenko, V., Levchuk, S., Bugai, D., van Meir, N., Simonucci, C., Martin-Garin, A., 2012. Radionuclide migration in the experimental polygon of the Red Forest waste site in the Chernobyl zone – Part 1: characterization of the waste trench, fuel particle transformation processes in soils, biogenic fluxes and effects on biota. Appl Geochem 27 (7), 1348–1358, 2012.
[18] Leifermann, L., Weiss, M., Chyzhevskyi, I., Dubchak, S., Hanemann, P., Raiwa, M., Schulz, W., Steinhauser, G., Weissenborn, T., Walther, C. 2023. Localisation, isolation and leaching of single hot particles from various environmental matrices in the vicinity of the Chernobyl nuclear power plant. [book auth.] Nicholas Evans. Environmental Radiochemical Analysis VII. 1st ed. La Vergne: RSC, 2023, pp. 1–18.
[19] Magill, J., Pfennig, G. and Galy, J. 2018. Karlsruher Nuklidkarte. 10. Auflage. Karlsruhe; Lage: Nucleonica GmbH;Marktdienste Haberbeck GmbH, 2018. p. 72. 9783943868500.
[20] Makarova, T.P., Bibichev, B.A., Domkin, V.D., 2008. Destructive analysis of the nuclide composition of spent fuel of WWER-440, WWER-1000, and RBMK-1000 reactors. Radiochemistry 50, 414–426, 2008.
[21] Ohm, D. 2023. Berechnung isotopischer Fingerprints verschiedener Reaktortypen für die nukleare Forensik. Leibniz University Hannover: IRS, 2023.
[22] Raiwa, M. 2022b. Zerstörungsfreie Analyse von Kernbrennstoffpartikeln aus der Sperrzone Tschernobyls. s.l.: Hannover: Institutionelles Repositorium der Leibniz Universität Hannover, 2022.
[23] Raiwa, M., Büchner, S., Kneip, N., Weiß, M., Hanemann, P., Fraatz, P., Heller, M., Bosco, H., Weber, F., Wendt, K., Walther, C., 2022. Actinide imaging in environmental hot particles from Chernobyl by rapid spatially resolved resonant laser secondary neutral mass spectrometry. Spectrochim Acta Part B: Spectrosc 190, 106377, 2022.
[24] Raiwa, M., Savina, M., Shulaker, D.S., Roberts, A., Isselhardt, B., 2024. Zirconium analysis in microscopic spent nuclear fuel samples by resonance ionization mass spectrometry. JAAS, 2024.
[25] Rest, J., 1989. Validation of mechanistic models for gas precipitation in solids during postirradiation annealing experiments. J Nucl Mater 168, 243–261, 1989.
[26] Rest, J., Cooper, M.W.D., Spino, J., Turnbull, J.A., van Uffelen, P., Walkrt, C.T., 2019. Fission gas release from UO2 nuclear fuel: a review. J Nucl Mater 513, 310–345, 2019.
[27] Salbu, B., Kashparov, V., Lind, O., Garcia-Tenorio, R., Johansen, M., Child, D., Roos, P., Sancho, C., 2018. Challenges associated with the behaviour of radioactive particles in the environment. J Environ Radioact 186, 101–115, 2018.
[28] Salbu, B., Krekling, T., Lind, O.C., Oughton, D.H., Drakopoulos, M., Simionovici, A., Snigireva, I., Snigirev, A., Weitkamp, T., Adams, F., Janssens, K., Kashparov, V. A. 2001. High energy X-ray microscopy for characterisation of fuel particles. Nuclear Instruments and Methods in Physics Research Section A: Accelerators, Spectrometers, Detectors and Associated Equipment. 2001, Vols. 467-468, pp. 1249–1252.
[29] Savina, M.R., Shulaker, D., Isselhardt, B., Brennecka, G., 2023. Rapid isotopic analysis of uranium, plutonium, and americium in post-detonation debris simulants by RIMS. J Anal Spectrom 38 (6), 1205–1212, 2023.
[30] UNSCEAR. 1988. UNSCEAR 1988 Report. [ed.] United Nations Scientific Committee on the Effects of Atomic Radiation. 1988. p. 647.
[31] USSR and Energy, State Committee on the Utilization of Atomic, 1986. The accident at the chernobyl nuclear power plant and its consequences. Vienna: S N 1986, 532.
[32] van Eerten, D., Raiwa, M., Hanemann, P., Leifermann, L., Weissenborn, T., Schulz, W., Weiß, M., Shulaker, D., Boone, P., Willingham, D., Thomas, K.,

Sammis, B., Isselhardt, B., Savina, M., Walther, C., 2023. Multi-element isotopic analysis of hot particles from Chornobyl. J Hazard Mater 452, 131338.
[33] Wakabayashiy, T., Mochizuki, H., Kitahara, T., 1987. Analysis of chernobyl reactor accident (I). s.l. Nucl Eng Des 103, 1987.
[34] Walker, C.T., Bremier, S., Portier, S., Hasnaoui, R., Goll, W., 2009. SIMS analysis of an UO2 fuel irradiated at low temperature to 65MWd/kgHM. J Nucl Mater 393 (2), 212–223, 2009.